



## THE VERTICAL, ROTATIONAL AND LATERAL RESPONSE OF UNBONDED FIBER REINFORCED ELASTOMERIC ISOLATORS

Yasser, Al-Anany  
Ph.D. Candidate, McMaster University, Canada.

Michael, J. Tait  
Professor, JNE Consulting Chair in Design, Construction, and Management in Infrastructure Renewal McMaster University, Canada

Torrie, Mark  
M.Eng, P.Eng Bridge Engineer, Associated Engineering, Canada.

Alexander, Sciascetti  
M.A.Sc. Student, McMaster University, Canada.

### ABSTRACT

Bridge structures often experience damage during an earthquake, which is one of the most devastating types of natural disasters. Base isolation can be employed to mitigate earthquake-induced damage. The main concept of base isolation is to reduce the seismic demand on the structure by shifting its fundamental time period away from the predominant periods associate with earthquakes. Base isolation involves placing horizontally flexible isolators between the bridge superstructure (i.e. deck/girder) and the substructure (i.e. pier/column). There are two main types of seismic isolators: (1) elastomeric, and (2) sliding. A fiber reinforced elastomeric isolator (FREI) is a particular type of reinforced elastomeric isolator. In an FREI the steel reinforcement used in a traditional elastomeric isolator is replaced with fiber fabric, which results in a reduction in the weight and potentially the manufacturing cost. FREI can be either bonded (B-FREI) or unbonded (U-FREI) to the substructure and superstructure. This paper investigates the behaviour of U-FREI under combined vertical, rotational, and lateral loading, as bridge bearings are expected to experience this combination of loads. Accordingly, the test program includes different vertical loads, angles of rotation, as well as a number of lateral sinusoidal input motions varying in both frequency and amplitude. The objective of this study is to investigate the response of U-FREI under serviceability and extreme loading conditions. The findings of this paper also address the feasibility of using U-FREI as bridge bearings/isolators.

Keywords: bridge structures; base isolation; fiber-reinforced; experimental testing; rotational response

### 1. INTRODUCTION

The observed number of bridge failures during major seismic events, including the 1971 San Fernando, 1989 Loma Prieta, and 1994 Northridge, California earthquakes and the 1995 Kobe, Japan, and 1999 Chi-Chi, Taiwan earthquakes, confirms the importance of seismic design (Moustafa and Mosalam 2015(a&b)). As such, bridge engineers are constantly searching for innovative techniques and devices that are able to prevent fatalities and mitigate damage. This can be accomplished by either increasing the capacity of the structure or decreasing the seismic demand placed on the structure. The 1995 Kobe, Japan earthquake demonstrated that increasing bridge capacity is not always effective (Jangid 2004). However, employing the technique of base isolation to decrease the seismic demand placed on the structure reduces the seismic forces and accelerations placed on the superstructure and substructure, as well as redistributes the seismic forces between the substructure of the bridge (i.e. piers and abutment).

Base isolation of a bridge is based on the concept of isolating the superstructure (i.e. deck and girder) from ground motions induced in the substructure (i.e. piers and abutments). This can be achieved by introducing elements, known as isolators, having low horizontal stiffness, between the superstructure and substructure. Because these elements serve as the only link between the superstructure and substructure, they must also be able to support the vertical loads and accommodate the rotations induced in the superstructure by the applied loads (mainly the dead and live loads). The low lateral stiffness of the isolators shifts the natural period of the structure to the displacement sensitive response region, where the inertial forces and accelerations are significantly reduced. This reduction in acceleration can be in order of 3, which allows the bridge to be resilient and respond in the elastic region during the design earthquake motion (Constantinou et al. 2010). This significant reduction in the seismic demand is why base isolation has been employed in thousands of bridges worldwide (Buckle 2006).

There are two main types of seismic isolators are: (1) sliding, and (2) elastomeric. The sliding isolation system is based on the transmission of lower shear forces to the structure through isolators with a low friction coefficient. Sliding isolation systems are typically either pure friction systems or friction pendulum systems (Girish and Praneesh 2013). Elastomeric isolators, which are the most widely used type of seismic isolator, consist of flexible elastomer layers reinforced by steel plates. There are three main types of steel reinforced elastomeric isolators (SREI), low-damping natural rubber (LDR) isolators, lead-plug rubber (LPR) isolators and high-damping natural rubber (HDR) isolators. However, due to the high cost and weight of SREI, their usage had been limited to high-importance high-value structures (Kelly and Konstantinidis 2007).

A relative significant reduction in both weight and potential manufacturing costs are possible if fiber fabrics are used to reinforce the elastomeric isolators instead of steel. The fiber reinforcement can be bonded to the elastomer using a cold-vulcanized bonding compound without the need of a mold. Furthermore, individual isolators can be cut from large sheets using a standard band-saw. An increase in the flexural flexibility of the reinforcement is another advantage gained from eliminating the rigid steel end plates and replacing the steel reinforcement with fiber material. Moreover, the interaction between fibers within the reinforcement provides a new source of energy dissipation in addition to the intrinsic damping of the elastomer.

Fiber reinforced elastomeric isolators (FREI) can be classified as either bonded, partially bonded, or unbonded according to the employed connection between the isolator and the contact surfaces of the substructure and the superstructure. This paper will focus on the behaviour of unbonded FREI (U-FREI). As a result of the unbonded boundary conditions and lack of flexural rigidity of the fiber fabric reinforcement, this type of isolator can experience *rollover* and *lift-off* under lateral and rotational deformations, respectively, as shown in Fig. 1.

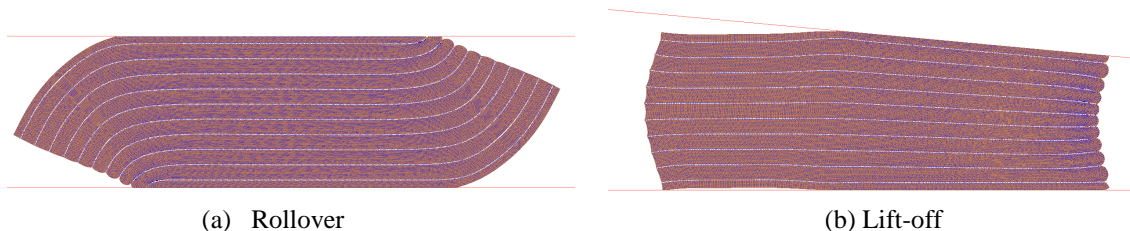


Fig. 1: (a) Lateral and (b) rotational deformation patterns of an U-FREI

The main objective of this paper is to experimentally investigate the response of U-FREI when subjected to lateral, vertical, and rotational deformations/load levels that are expected to occur over the lifetime of a bridge structure. Additionally, the resulting stress/strain states in the U-FREI under the loads considered in the experimental study will be evaluated using three-dimensional finite element modelling (FEM). The parameters varied during this study are:

1. Mean vertical stress ( $\sigma_v$ ) = 2, 4, 6, 8 and 10 MPa.
2. Static rotation ( $\theta$ ) = 0, 0.015, 0.03 radians.
3. Dynamic lateral cyclic displacement amplitude ( $U_L$ ) = 0.25, 0.5, 1.0, 1.5, and 2.00  $t_r$  (total rubber thickness).

## 2. EXPERIMENTAL TESTING

### 2.1 Test-rig

The experimental program was conducted using the 3 degree-of-freedom (3DOF) bearing test apparatus, shown in Fig. 2, which was constructed in the Applied Dynamics Laboratory (ADL) at McMaster University for the primary purpose of testing seismic isolators. This test apparatus was designed to be capable of applying the vertical, rotational, and lateral movement (simultaneously or independently) via displacement or load control. The main components of the test apparatus are the loading beam, pedestal, and reaction frame. The reaction frame is comprised of stiffeners placed at the actuator reaction points, pedestal and vertical reaction arm. The main pedestal supports a thick bottom platen. A cold rolled plate is attached to the top of the bottom platen and serves as the lower contact support.

Loads and deformations are applied to the isolator specimen through a cold rolled steel plate attached at the mid-span of the loading beam. A total of three hydraulic actuators are also attached to the loading beam. The two vertical actuators, located at either end of the loading beam, are used to apply the vertical loads and rotational deformations on the test specimen. The lateral actuator, which is attached to one end of the loading beam, is used to apply lateral loads/deformations. Roller guides are located on both sides of each end of the loading beam to ensure lateral stability. Additionally, two three-axis load cells are used to measure the vertical and lateral loads. The vertical deflection of the isolators during loading (vertical and lateral cyclic) are measured using four laser displacement transducers attached at the four sides of the loading platen. In this study all the tests were conducted at room temperature and the data was recorded at 200 Hz.

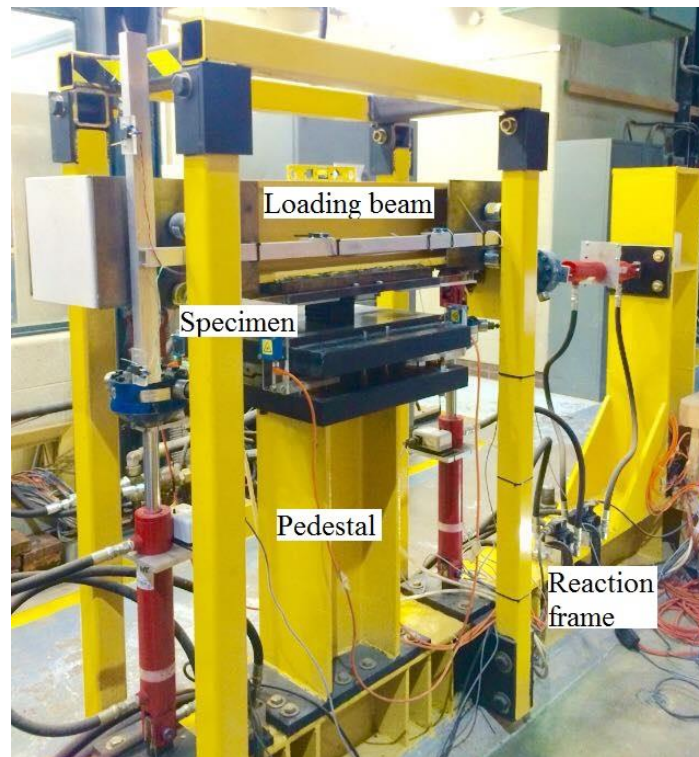


Fig. 2: 3D testing machine

### 2.2 Specimens and testing program

A FREI specimen with physical dimensions of 70.0 mm x 70.0 mm x 22.4 mm was cut from a laminated fiber reinforced elastomeric sheet. The specimen comprised of 5 interior natural rubber layers with a thickness of 3.19 mm and 2 cover layers with a thickness of 1.58 mm. Thus, the total rubber thickness ( $t_r$ ) was approximately equal to 19.05 mm. The reinforcement sheets used were a plain weave bi-directional carbon fiber with a thickness of 0.25

mm. The shape factor,  $S$ , defined as the ratio between loaded area and the area free to bulge, was determined to be 5.50, which lies in between the common range of elastomeric bearings employed in bridges structures (i.e.  $3 < S < 8$ ) (Stanton 2007). Additionally, the aspect ratio,  $AR$ , defined as the ratio between the total length/width and total height, was determined to be 3.40.

## 2.3 Phase I: vertical behaviour

### 2.3.1 Effects of axial loads levels

Seismic isolators must possess sufficient vertical stiffness in order to adequately resist and transmit gravity loads from the superstructure to the substructure. This section investigates the vertical response of the U-FREI under a range of axial loads. The vertical testing was conducted by loading the specimen under load control up to the desired level of axial load. Once the target axial load,  $P$ , was reached three fully reversible cycles with amplitude  $\pm 20\% P$  at a loading rate of 0.2 Hz were applied. The vertical stiffness was determined from the measured response using the following relation (ISO 2010)

$$[1] \quad \frac{F_{v,\max} - F_{v,\min}}{\Delta_{v,\max} - \Delta_{v,\min}}$$

where  $F_{v,\max}$ ,  $F_{v,\min}$ ,  $\Delta_{v,\max}$ ,  $\Delta_{v,\min}$  are the minimum and maximum vertical forces and displacements, respectively, observed over the third loading cycle. Figure 3 shows the results of the vertical testing completed on the test specimens. It can be observed that an increase in the amplitude of the applied axial load resulted in a nonlinear increase in the vertical stiffness of the isolator. A primary reason for this behaviour is due to the initial lack of straightness of the individual fibers (Kelly 2008). As a vertical load is applied, the lateral bulging of the elastomer creates a tensile stress in the fiber reinforcement that pulls the individual fibers taut, which consequently results in a higher vertical stiffness as the restraint on the elastomeric layers is increased. Additionally, the vertical damping ratio ( $\zeta_v$ ), which was calculated based on the area within the hysteresis loops, was found to be approximately 1%. Finally, the tested isolator exhibited vertical frequencies corresponding to the applied axial load ranging from 17 to 29 Hz, which is considered satisfactory for seismic isolation applications.

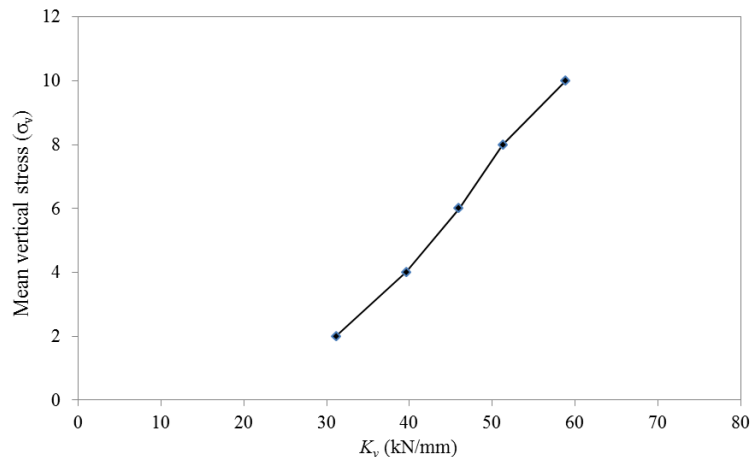


Fig. 3: The influence of axial load amplitude ( $P$ ) on the vertical stiffness ( $K_v$ ) of the isolator

### 2.3.2 Effects of static rotations

Bridge superstructures are subjected to rotational deformations due to dead loads, live loads, and/or geometric imperfections of eccentricities. This section investigates the effect of bridge deck/girder rotations on the vertical stiffness of the isolator. Static rotations of 0, 0.01, 0.02, 0.03 radians were considered in the study. The isolator was vertically loaded in the same manner described in the previous section. However, the static rotation was applied before the three fully reversible vertical cycles were applied to the isolator. The effect of static rotation on the vertical stiffness of isolators is shown in Fig. 4. Static rotations can lead to a loss of contact area between the isolator

and the supports, which is expected to lead to a decrease in vertical stiffness as observed at lower applied vertical loads. However, it is postulated that the insignificant change in vertical stiffness under higher levels of applied vertical loads is primarily due to the increase in the vertical stresses on one side of the isolator (Al-Anany and Tait 2015b), which also results in an increase in the fiber tensile stresses. The increased level of tension in the fiber reinforcement is expected to increase in vertical stiffness and as a result the reduction due to the loss of contact area is mitigated (Al-Anany and Tait 2016a)

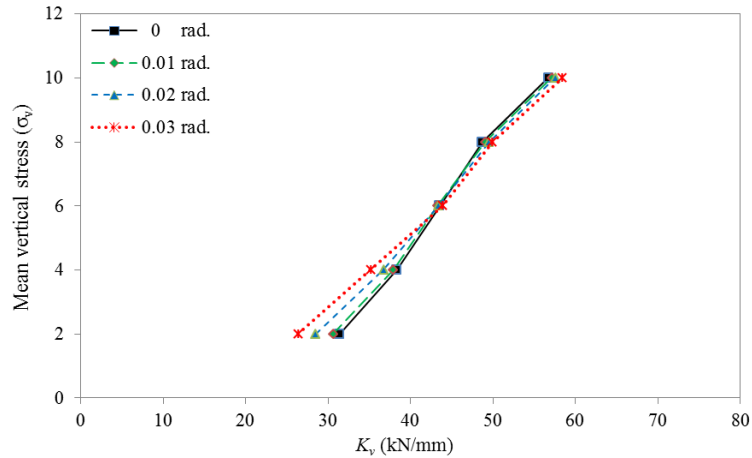


Fig. 4 The influence of axial load amplitude (P) and static rotation ( $\theta$ ) on the vertical stiffness ( $K_v$ ) of the isolator

### 2.3.3 Effects of lateral offsets

Bridge superstructures are subjected to various temperatures throughout the year, which results in expansion and contraction of the deck/girder. Additionally, lateral movement may occur due to creep and shrinkage, elastic shortening due to prestressing and traffic loading (AASHTO-LRFD 2012). However, the maximum amplitude of this lateral movement is specified/ limited by bridge design codes (ex. CSA 2014) to be less than a value of  $0.50 t_r$ . The objective of this section is to present the influence of lateral offset on the vertical stiffness of the isolator. A lateral offset is the lateral displacement applied to the specimen after applying the vertical load but prior to cycling the load vertically on the specimen. Figure 5 presents the effect of lateral offset on the vertical stiffness of a U-FREI. It can be observed that the lateral offset has no significant effect on the vertical stiffness. A recent study by Al-Anany and Tait (2016b) has shown that the vertical stiffness of the isolator can be maintained up to a lateral offset of  $1.50 t_r$ .

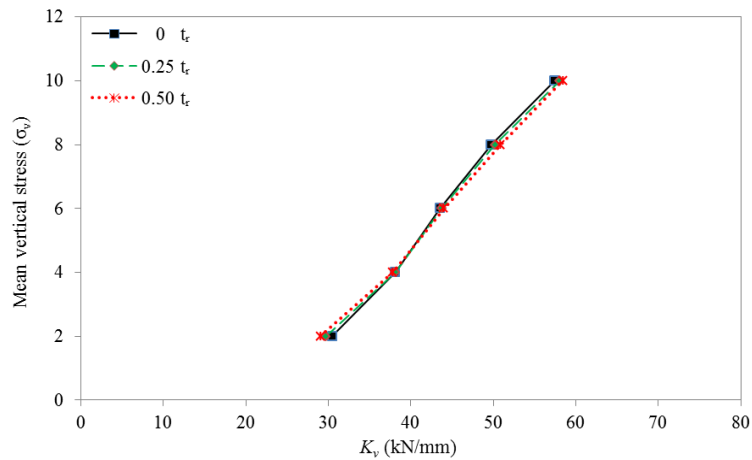


Fig. 5: The influence of axial load amplitude (P) and lateral offset ( $\Delta_L$ ) on the vertical stiffness ( $K_v$ ) of the isolator

## 2.4 Phase II: rotational behaviour

The rotational behaviour of an isolator should be evaluated to ensure the ability of the isolator to accommodate the cyclic rotational deformations expected during the lifetime of the bridge. This section aims to investigate the rotational response of the isolator when subjected to quasi-static cyclic rotations with amplitudes of 0.01, 0.02 and 0.03 radians. The isolators were initially loaded up to the target axial loads, under load control, before cyclic rotations were applied under displacement control. The moment-rotational response of the isolator under three different levels of axial loads is shown in Fig. 5. It can be observed that the rotational response of the isolator exhibits a softening type behaviour due to lift-off as the rotational amplitude is increased under smaller axial load levels. As the amplitude of the applied axial load is increased, lift-off is delayed or completely prevented and the isolator exhibits a near linear rotational response (Al-Anany and Tait 2015b).

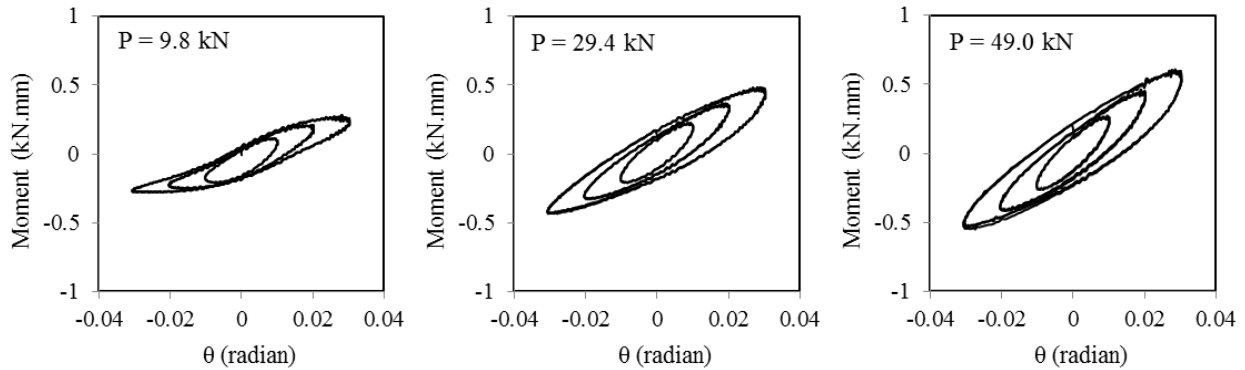


Fig. 5: Moment-rotation response of the isolator

## 2.3. Phase III: lateral behaviour

The lateral force-displacement behaviour of U-FREI under three different vertical loads is shown in Figure 6. Each lateral test, which consisted of three cycles at five ascending normalized displacement amplitude ( $\Delta_L/t_r$ ) values of 0.25, 0.50, 1.00, 1.50, and 2.00  $t_r$ , was conducted under a lateral loading rate of 76 mm/sec.

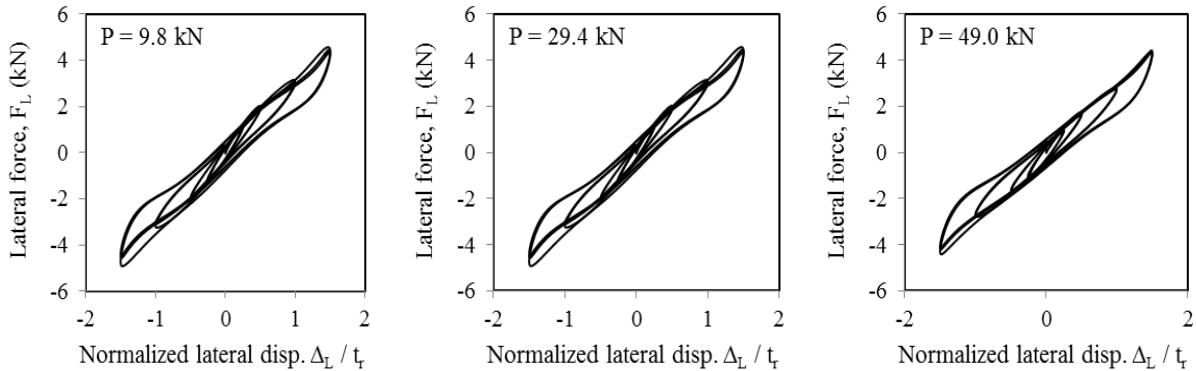


Fig. 6: Lateral response of the isolator

As shown in Fig. 6, the isolator experiences a reduction in the lateral stiffness as the lateral displacement is increased. This is due to rollover, which results in a reduction in the effective shear area (Osgooei P. 2014&2015, Van Engelen N. et al. 2014&2015). It can also be seen that the level of applied axial load had a negligible effect on the lateral response of the isolators.

### 3. FINITE ELEMENT MODELLING

#### 3.1 Model-description

Three-dimensional finite element (FE) modelling was carried out for the analysis of the considered U-FREI under vertical and rotational loading. The primary goal of the FE-analysis is to evaluate and assess the resulting stress and strain state within the isolator when subjected to the considered axial loads and angles of rotation applied in the experimental study. FE analyses were completed using the commercially available general-purpose finite element programs, MSC Marc. The elastomer was modelled with an eight-node isoparametric quadrilateral brick element. The hyperelastic Neo-Hookean material model was used to represent the elastomer. This model is defined by two parameters representing the bulk modulus ( $K_e$ ) and the shear modulus ( $G_e$ ) of the elastomer material, which correspond to an elastic modulus of 2.58 MPa and a Poisson's ratio of 0.4998. The reinforcement material was modelled using a linear elastic isotropic material, which is typically defined by two constants: the elastic modulus ( $E_f$ ) and Poisson's ratio ( $\nu_f$ ) of the fiber. The material properties considered in the FE model were determined from experimental tests and are shown in Table 1.

Table 1: Material properties

Elastomer	Fiber
Shear Modulus, $G_e = 0.86$ MPa	Elastic Modulus, $E_f = 20$ GPa
Bulk Modulus, $K_e = 2000$ MPa	Poisson's ratio, $\nu_f = 0.20$

Two rigid wires were used to model the top and bottom contact support surfaces. The upper rigid wire had a control node with two degrees of freedom one in the vertical direction and one in the rotational direction. The lower rigid wire was constrained from any movement. Additional modelling details can be found elsewhere (Al-Anany and Tait 2015a, 2015b).

#### 3.2 Results and discussions

This section presents the vertical stresses ( $\sigma_{22}$ ) that developed in the isolator under a range of axial loads and angles of rotation. Fig. 7 presents the normalized stress contours ( $\sigma_{22} / \sigma_v$ ) under values of average applied stress ( $\sigma_v$ ) of 2, 6, and 10 MPa. The stress contours are shown within the isolator by taking a section along the centre of the isolator. It can be observed that the magnitude of ( $\sigma_{22}$ ) is essentially constant in the vertical direction with a normalized peak value of 2.00, which is expected for a square elastomeric isolator.

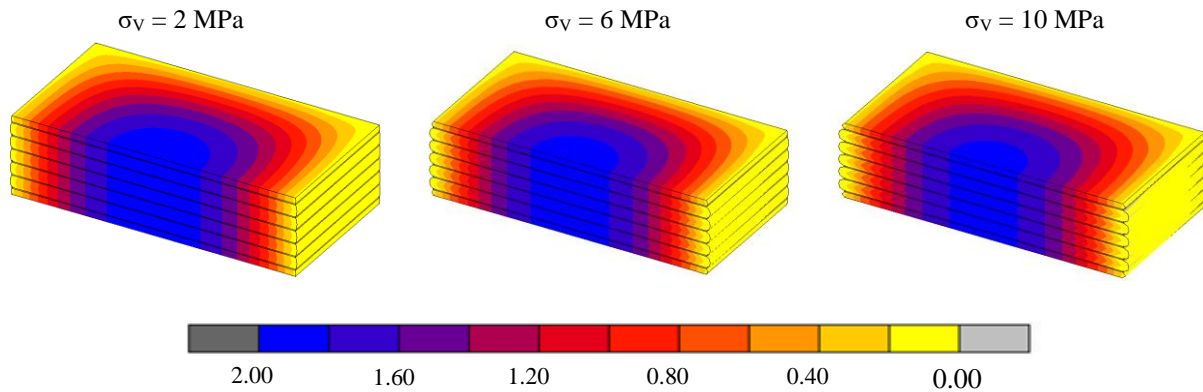


Fig. 7: Normalized stress contours ( $\sigma_{22} / \sigma_v$ )

Figures 8 and 9 show the evolution of normalized stress distribution ( $\sigma_{22} / \sigma_v$ ) within the isolator under average compressive stress ( $\sigma_v$ ) values of 2 and 10 MPa, respectively. As shown in Figs. 8 and 9, the normalized stresses are presented at different angles of rotation ( $\theta$ ) = 0, 0.01, 0.02, and 0.03 radians. It can be observed that the magnitude of compressive stresses that developed in the isolator increase as the applied angle of rotation is increased. An

increase in the applied angle of rotation leads to lift-off, which consequently results a reduction in the loaded area and a corresponding increase in the compressive stress.

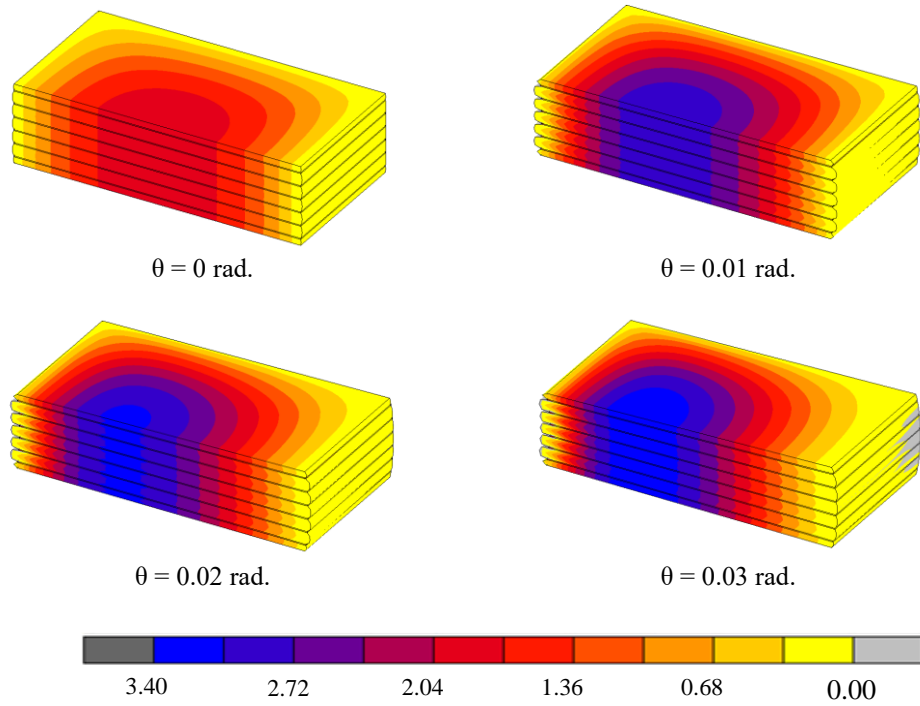


Fig. 8: Evolution of Normalized stress contours ( $\sigma_{22} / \sigma_v$ ) under different angles of rotation and average compressive stress ( $\sigma_v$ ) of 2 MPa

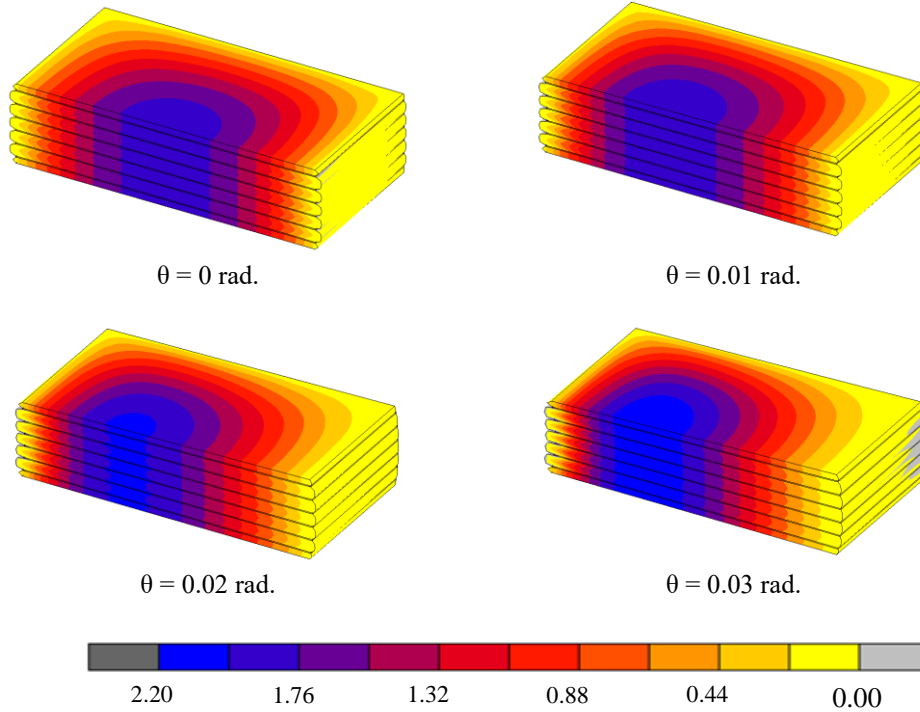


Fig. 9: Evolution of Normalized stress contours ( $\sigma_{22} / \sigma_v$ ) under different angles of rotation and average compressive stress ( $\sigma_v$ ) of 10 MPa

Furthermore, the increase in the peak stress is more significant under lower levels of compressive stresses, which is also related to the occurrence of lift-off. Under low compressive stress (i.e.  $\sigma_v=2\text{MPa}$ ), lift-off occurs (i.e. reduction in the loaded area), which results in a higher increase in the compressive stresses. However, under higher levels of compressive stress (i.e.  $\sigma_v=10\text{MPa}$ ) the occurrence of lift-off is delayed, and as a result the applied axial loads continue to be resisted by the full contact area. Additionally, the development of tensile stresses in the U-FREI is negligible because lift-off is permitted for this type of unbonded isolator. Thus, lift-off allows this unbonded isolator to separate from the support surfaces under excessive rotational deformation; resulting in the development of only compressive and shear forces between the unbonded isolator and the contact support surfaces.

#### 4. CONCLUSIONS

This paper presents test results of U-FREI when loaded in vertical, rotational, and lateral direction independently and in combination. Experimental testing and finite element modelling were both employed in this study. The square bearing investigated in this study had a plan area of 70 mm x 70 mm, shape factor of 5.50, and aspect ratio of 3.40. The main parameters varied during this study were the mean vertical stress ( $\sigma_v$ ) = 2, 4, 6, 8 and 10 MPa, static rotation ( $\theta$ ) = 0, 0.015, 0.03 rad., dynamic lateral cyclic displacement amplitude ( $U_L$ ) = 0.25, 0.5, 1.0, 1.5, and 2.00  $t_r$ . The main conclusions that can be drawn are:

1. The isolator exhibited a nonlinear increase in the vertical stiffness when the applied axially load level was increased.
2. The applied angle of rotation reduced the vertical stiffness of the isolator under low vertical loads. However, under high levels of vertical loads, and with any value for the angle of rotation, no significant change in vertical stiffness was observed.
3. A significant change in the vertical stiffness was observed in the U-FREI under the considered values of lateral offset (i.e.  $< 0.5 t_r$ ).
4. The amplitude of the vertical load applied on the isolator influenced the shape of the hysteresis loops, which also influenced the rotational stiffness.
5. The rate of increase in the compressive stresses developed within the isolator due to the rotational deformation was found to be higher under lower levels of vertical loads due to the rapid occurrence of lift-off.

#### ACKNOWLEDGEMENTS

This research was carried out as part of the mandate of the Centre for Effective Design of Structures (CEDs) at McMaster University and is partially funded by the Ontario Ministry of Economic Development and Innovation and by the Natural Sciences and Engineering Research Council of Canada (NSERC).

#### REFERENCES

- Al-Anany Y, Tait M. 2015a. A Study on the Rotational Behaviour of Bonded and Unbonded Fiber Reinforced Elastomeric Isolators, Proceedings of the 11th Canadian Conference on Earthquake Engineering, Victoria, British Columbia, Canada, 21-24 July.
- Al-Anany Y, Tait M. 2015b. A numerical study on the compressive and rotational behavior of fiber reinforced elastomeric isolators (FREI). *Composite Structures*, 133: 1249-1266.
- Al-Anany Y., Van Engelen, N. and Tait M. 2016a. An experimental investigation on the vertical and lateral behaviour of unbonded fiber-reinforced elastomeric isolators, *Engineering Structures*, under review.
- Al-Anany Y. and Tait M. 2016b. An experimental study of the vertical and rotational behaviour of unbonded fiber-reinforced elastomeric isolators (U-FREI) for bridge applications, *ASCE Journal of Bridge Engineering*, under review.
- AASHTO. 2012. American Association of State Highway and Transportation Officials. LRFD Bridge Design Specifications, Washington, D.C.

- CAN/CSA-S6-14. 2014. Canadian Highway Bridge Design Code. Canadian Standard Association. Ontario.
- Constantinou M., Kalpakidis I., Filiatrault A., and Ecker Lay R. 2010. *LRFD-based analysis and design procedures for bridge bearings and seismic isolators*. Report No. MCEER-11-0004, Multidisciplinary Center for Earthquake Engineering Research, University at Buffalo, State University of New York, Buffalo, New York.
- Girish M. and Pranesh M. 2013. Sliding Isolation Systems: State-of-the-Art Review. *IOSR Journal of Mechanical and Civil Engineering (IOSR-JMCE)*. 02/2013; 6:30–35.
- ISO. 2010. *Elastomeric seismic-protection isolators*. ISO 22762, Geneva.
- Jangid R. 2004. Seismic response of isolated bridges. *ASCE Journal of Bridge Engineering*, 9(2):156–166.
- Kelly J. and Konstantinidis D. 2007. Low-cost seismic isolators for housing in highly seismic developing countries. *ASSISI 10<sup>th</sup> World conference on seismic isolation, energy dissipation and active vibrations control of structures*, Istanbul, Turkey.
- Kelly J. 2008. Analysis of the run-in effect in fiber-reinforced isolators under vertical load. *Journal of Mechanics of Materials and Structures*, 3(7):1383–401.
- Moustafa M. and Mosalam K. 2015a. *Structural Behavior of Column-Bent Cap Beam-Box Girder Systems in Reinforced Concrete Bridges Subjected to Gravity and Seismic Load, Part I: Pre-test Analysis and Quasi-Static Experiments*. Pacific Earthquake Engineering Research Center, PEER, Berkeley, California; 2015/09.
- Moustafa M. and Mosalam K. 2015b. *Structural Behavior of Column-Bent Cap Beam-Box Girder Systems in Reinforced Concrete Bridges Subjected to Gravity and Seismic Load, Part II: Hybrid Simulation and Post-Test Analysis*. Pacific Earthquake Engineering Research Center, PEER, Berkeley, California; 2015/10.
- MSC. Marc. Santa Ana, CA: MSC Software Corporation; 2013.
- Osgoee P., Tait M., and Konstantinidis D. 2014. Finite element analysis of unbonded square fiber-reinforced elastomeric isolators (FREIs) under lateral loading in different directions. *Composite Structures*. 113: 164-173.
- Osgoee P., Van Engelen, N., Konstantinidis D., and Tait M. 2015. Experimental and finite element study on the lateral response of modified rectangular fiber-reinforced elastomeric isolators (MR-FREIs). *Engineering Structures*. 85: 293-303.
- Stanton J, Roeder C, Mackenzie-Helnwein P, White C, Kuester C., and Craig B. 2007. *Rotation Limits for Elastomeric Bearings*. Report No. NCHRP 596, Transportation Research Board, National Cooperative Highway Research Program, Washington, D.C.
- Van Engelen N., Tait, M., Konstantinidis D. 2014. Model of the Shear Behavior of Unbonded Fiber-Reinforced Elastomeric Isolators. *ASCE Journal of Structural Engineering*. 141(7): 04014169.
- Van Engelen, N., Osgoee P., Tait M., and Konstantinidis D. 2015. Partially bonded fiber-reinforced elastomeric isolators (PB-FREIs). *Structural Control and Health Monitoring*. 22(3): 417-432.